Sustainable Marine Structures
https://journals.nasspublishing.com/sms

REVIEW

Parameterizing the Sea Surface Drag Coefficient over Aiyetoro in Ilaje Local Government Area, Ondo State, Southwestern Nigeria

Adekunle Ayodotun Osinowo [1]* , Lateef Adesola Afolabi [2] , Pasquale Contestabile [2] , Segun Ohunayo Ekudehinwa [3], Gideon Efeoghene Ovwuwonye [1]

[1] *Department of Marine Science and Technology, Federal University of Technology, Akure 340252, Nigeria*

[2] *Department of Engineering, University of Campania Luigi Vanvitelli, 81031 Aversa, Italy*

[3] *Department of Meteorology, Nigerian Maritime University, Okerenkoko 332105 Nigeria*

ABSTRACT

Ocean surface waves and upper sea circulation are primarily propelled by wind force and are usually expressed in terms of sea surface drag coefficient (c_d) that increases with sea surface roughness and wind speed. This work discussed the c_d parameterization at Aiyetoro, Ilaje Local Government Area, Ondo State, Southwestern Nigeria, to quantify the exchange of momentum in this region, The dependence of c_d on some one hourly averaged variables sourced from ERA5 Reanalysis over a 71 year period (1950–2020) was clearly analysed. Results of the monthly mean and variability of cd and u10 over the study area showed that November had the lowest monthly mean cd and u10, with values of 0.000825 and 3.38 m/s, respectively, and August had the highest values of 0.001031 and 5.66 m/s, respectively. Furthermore, the cd variability is lowest (63.24%) in November and highest (106.35%) in August. The variability for u10 is lowest in March (198.18%) and greatest in October (304.37%). For the study location, five parameterizations, were statistically evaluated for the predictive power of c_d on an annual, seasonal and monthly basis. Furthermore, the c_d showed improved performance when using monthly values than when using annual and seasonal values. The equations yielded better performance in the wet season than in the dry season.

Keywords: Era5 Reanalysis Data; Sea Surface Drag; Parameterization; Wind-Sea Interaction; Wave Dynamics; Momentum

*CORRESPONDING AUTHOR:
Adekunle Ayodotun Osinowo, Department of Marine Science and Technology, Federal University of Technology, Akure 340252, Nigeria; Email: aaosinowo@gmail.com

ARTICLE INFO
Received: 11 April 2025 | Revised: 6 May 2025 | Accepted: 26 May 2025 | Published Online: 21 July 2025
DOI: https://doi.org/10.36956/sms.v7i3.1989

CITATION
Osinowo, A.A., Afolabi, L.A., Contestabile, P., et al., 2025. Parameterizing the Sea Surface Drag Coefficient over Aiyetoro in Ilaje Local Government Area, Ondo State, Southwestern Nigeria. Sustainable Marine Structures. 7(3): 43–62. DOI: https://doi.org/10.36956/sms.v7i3.1989

1. Introduction

The circulation of the upper sea and ocean surface waves are primarily propelled by wind force acting on the ocean surface. For satellite remote sensing of global wind field, oceanic and atmospheric processes, and modeling, it is imperative to accurately estimate wind stress. Wind stress has been extensively investigated through observations and numerical models over the past few decades because of its crucial importance in comprehending and modeling the processes between the air and sea [1]. Wind force over the ocean surface is usually expressed in terms of c_d. Empirical determination of the variables in the equation is achieved by fitting field data to a curve thus, allowing c_d to be expressed as a function of the 10m wind speed (u_{10}). Many of the c_d equations are represented as linear functions, especially when u_{10} ranges from 7 to 20 m/s. This note aims to lay the groundwork for a linear parameterization of c_d and to offer a consistent method for resolving discrepancies among various linear parameterization forms.

Some early researches suggest that c_d is highly dependent on wind speed and introduces numerous parameterization techniques in terms of average wind speed only. The significant impact of ocean surface waves on wind stress is noted. According to the research [2], c_d should be parameterized using the wave age (c_p/u_{10} or β), since they demonstrated a reliance on the rate of wind wave growth. The research [3] also suggested parameterizing c_d using the significant wave height (*hs*), peak wavelength (*lp*), or wave steepness (δ).

Numerous c_d parameterization approaches have been created in the last few decades based on data from ship trips, buoys, and towers. The wind speed and wave steepness were proposed by the research [3] as ways to parameterize c_d. According to the research [2], there are notable differences between Open Ocean and shallow and coastal seas. They suggested using distinct c_d parameterizations for the two types of waters. According to the research [4], it would be better to explain the c_d, using the wind-sea Reynolds number (R_B). Other parameterizations are those of [5] and [6], which depend on R_B, δ and $u_{10.}$

It is crucial to know that the c_d is an excellent tool for determining the aerodynamic friction between air and sea. The research [7] derived a regression of the relationships between the c_d and wind speed across various wind ranges, utilizing an observational dataset comprising 5941 estimates of mean flow and fluxes from 11 aircraft turbulent measurements over the sea surface. They discovered that the c_d behaves as a power function of wind speed over a smooth sea surface when the speed is 4.5 ms^{-1} or lower, and that it diminishes as wind speed increases; and for a rough sea surface, when the wind speed exceeds 4.5 ms^{-1} but is no greater than 10.5 ms^{-1}, the c_d rises in direct proportion to the increase in horizontal wind speed; when wind speed exceeds 10.5 ms^{-1} but does not go beyond 33.5 ms^{-1}, the ocean surface c_d varies in a parabolic manner as wind speed rises; the c_d remains constant when wind speed exceeds 33.5 ms^{-1}.The threshold for saturated wind speed, derived from the c_d regression, is 23 ms^{-1}. The turbulent heat transfer coefficient and the water vapor transfer coefficient were also examined for parameterizations.

The parameterizations of sea-surface roughness relative to wave age, was studied by the research [8]. They found that the peak phase speed (cp) is a germane parameter to evaluate c_d. Using the same wave age, c_d increases with rising cp. They computed fricition velocity and suggested that the frequency bandwidth and spectral width of the wave spectrum are better parameters than the usual wind speed and wave age used in parameterizing c_d. A sea surface c_d is applied by the research [9] in the computation of air–sea momentum flux under great wind speeds. They observed that wave age plays a vital part in computing c_d. With wave age greater than 0.4, c_d declines with the wave age. Also, with wave age lesser or equal to 0.4, c_d rises with wave age at low and moderate wind velocities, but declines with wave age at great wind velocities

The research [10] used an observational dataset that consists of 806 estimates of the mean flow and fluxes from aircraft eddy-covariance measurements over the tropical Eastern Pacific to present the relationship between c_d and wind speed. Results show that the relationship between c_d and wind speed is parabolic.

From the data collected by eddy covariance systems in typhoons Hagupit and Chanthu, the research [11] studied the formulation of 10m wind speed, c_d, sea surface roughness length and friction velocity. Findings revealed parabolic patterns between friction velocity and c_d, and between 10 m wind speed and c_d. Results further showed exponential relationships between friction velocity and aerodynamic roughness length, and between 10m wind speed and sea roughness. They reported a critical friction velocity of 0.83 ms^{-1} and critical 10m wind speed of 23.69 ms^{-1}.

Regarding low to moderate wind speeds (u_{10} < 20 m/s) as mentioned by the research [12]), earlier observations revealed that c_d rises almost linearly with wind speed. In winds greater than 25 m/s, c_d flattens off or declines with rising wind speed [12,13]. The technique behind the reduction of c_d is not yet clear [6]. Also, of note is the act of interrelating the c_d to wind speed, which results to an unstable dimension [6]. By considering the effects of sea spray and wave development , a new parameterization of c_d which applies from low to extreme winds is suggested by the research [14]. It is found that in low-to-moderate wind conditions, aerodynamic roughness first rises and then declines with the rising wave age and in high wind situations, the c_d declines with the rising wind velocity as a result of the modification of the logarithmic wind profile following the impact of sea spray droplets produced by bursting bubbles. The c_d with the sea surface roughnesses get to their climax and vary under several wave states. Correspondingly, the decrease in c_d in strong winds decreases the rising friction velocity with rising wind velocity.

The impacts of c_d decrease in high winds as per TC intensity, particularly rapid intensification (RI) with lifetime maximum intensity (LMI) distribution, were studied by the research [15], by estimating the wind-dependent c_d-based ocean vertical mixing with energy budget. They concluded that c_d decrease may bring about RI and LMI bimodality.

The research [16] estimated c_d by a revised momentum budget and eddy covariance methods. Their estimates corresponded with in-situ measurements in low-to-moderate wind conditions and former laboratory studies in hurricane-force winds. The c_d is maximum at 2.6×10^{-3} and $u_{10} \approx 25$ ms^{-1} , which is in agreement with former laboratory findings by the research [17]. Their results stressed the essence for a recent drag formulation, which is based on field and laboratory data.

The wind-wave variables derived from WAVEWATCH III wave model simulation are used by the research [18] to calculate c_d. They involved default ST4 and ST6 parameterizations with ST1 and ST6 parameterizations engaged all together with the suggested c_d formulation. The findings got are intercompared with the NDBC buoys data. ST6 with the c_d spray revealed excellent temporal trend for all the buoys taken into account. Also, the suggested formulation showed good tracking of sharp peaks of wave height. It is described that the formulation relies on wind velocity and the age of the waves. This is particularly vital in hurricane situations. In a study by the research [19], the formulation of the c_d is developed using remotely sensed wind-wave products in tropical cyclones (TCs) and established for wave modeling by using WAVEWATCH-III (WW3) model. Five different c_d parameterization methods were evaluated by the research [20] for the simulation of two typhoon instances. They observed that the typhoon path and minimum sea level pressure were insensitive to c_d formulations. Findings of their study answered how the c_d affects the atmosphere and sea in typhoon process, and the extent to which they are affected, which have great improvements on simulation results.

The research [21] mentioned the development of the characteristics of ocean surface got by including measurements from microwave remote sensing. Essentially, the universal data of microwave monostatic and bistatic radar cross sections added to the assessment of sea surface roughness spectrum model, and measurements from microwave radiometer in tropical cyclones gave clarification with respect to the dependence on wind velocity on c_d and whitecap coverage.

The research [22] stated that the statistical performances of eight existing parameterizations of the c_d are evaluated using field observations across a wide range of wind and surface wave conditions. Evaluations of these field observations yield valuable insights into the momentum exchange across various sea states. To improve the representation of wind stress across var-

ious sea states compared to current methods, a new wave-dependent c_d parameterization is proposed. A nested-grid wave model for the northwest Atlantic (NWA) is used to investigate how well the new parameterization performs. The wind stress is used to simulate ocean surface waves over the NWA during a winter storm in March 2014, employing the new c_d parameterization as well as three existing ones. The outcomes of the model are juxtaposed with the measurements obtained from in-situ buoys and satellite altimeters that are available.

A new function for generating sea spray was developed by the research [23]. This function is based on both sea states (wave steepness or wave slope and β) and wind speed. When assessing rate of flow of momentum of droplets of sea spray in various wave conditions, this function was considered. Moreover, at low to moderate wind speeds, the effective c_d of the sea surface diminishes with rising β or wave slope. Given a challenge of collecting data on β and wave steepness at the same time, this study proposes a relationship formula that connects these parameters of wave state. Once the β surpasses 0.4, a strong relationship between β and wave slope is observed. As the velocity of wind escalates from low to greater levels, an obvious decrease in the effective sea surface c_d, accompanied by a rise in β is noticed. The wave slope reaches its peak when the age of the wave is under 0.4; at medium and smaller wind speeds, the effective ocean surface c_d increases with the age of wave. With rising wind velocity, the flux of momentum from the air rises. Simultaneously, the effective ocean surface drag declines as the age of the wave rises.

The research [24] conducted a systematic investigation into how surface waves affect wind stress, drawing on in-situ observations of air-sea fluxes and surface waves from three coastal tower-based platforms across different regions. A formulation that relies exclusively on wind speed was created for wind speeds ranging from 1 to 20 ms^{-1}. It could predict the attenuation of coastal c_d at a wind speed of 20 ms^{-1} and, when increased to 30 ms^{-1}, the saturation. Nonetheless, this wind-based method does not simulate the scatter of c_d in practice. A new wave-state-based formulation for c_d was suggested, which estimates both the widely spread c_d values and the saturation of c_d to a large extent. This was accomplished through a deeper examination of how wave states influence wind stress and by including the factors of the age of wave with the directionality of waves and wind in wind-dependent calculation. When compared to both the COARE and wind-based calculations, this new parameterization shows a reduction in RMSE of approximately 20% and 9%, respectively. The comparison between the newly parameterized c_d and the observed asymmetric c_d across various quadrants of tropical cyclones serves as further proof of the new parameterization's relevance. The wave-state-based parameterization method requires three parameters, which are u_{10}, β, and wave off-wind angle (θ), and is expected to be utilized in coastal regions.

The research [25] developed a physical scale experiment to measure c_d using wind profile and eddy covariance methods. This was done to tackle the problem of inadequate equations produced in inland lake models, which often lead to an underestimation of water velocity. Moreover, two experiments conducted on the lake were utilized to develop and evaluate a new c_d parameterization that is dependent on waves induced by wind. In a hydrodynamic model of the shallow Upper Klamath Lake in Oregon, USA, the wave-dependent c_d formula was applied to modify the driving force. Up to the critical u_{10} value of 1.6 m/s, which was 1.0–3.1 times previous empirical extrapolations in light winds, there was a negative correlation between the experimental c_d and wind velocity. The findings of the variation partitioning revealed that, when paired with wind factors, wave parameters accounted for almost 30% of the variation in c_d. At two sites, the modeled water velocity was more in line with the measurements, and the corrected wind stress field was spatially heterogeneous. In comparison to the original Upper Klamath Lake model, considerable main circulation and outer bank circulation were modeled alongside intensified surface vorticity. Ultimately, the wave-dependent c_d formula improved the surface flow field in the Upper Klamath Lake model and will contribute to better administration of ecosystems of lake. This finding is significant as the sea surface c_d is used to parameterize momentum and heat exchange between the atmosphere and ocean in climate models.

This enhances our understanding of climate variability and change, along with the precision of climate projections.

The c_d was parameterized using β by the research [26]. Initially used to signify the strength of wave breaking at the sea surface, R_B has found extensive application in research on the boundary layer between the ocean and atmosphere, including works on the gas exchange between air and sea, transfer of momentum, and sea spray creation [27]. Researchers recently clarified that the air-sea momentum flux is affected by both the age of wave and wave steepness [6]. The internal parameter representing wave stability is the wave slope. The age of the wave, which is an external variable, indicates how well wind can add energy to ocean surface waves.

With the progress of research, it has been uncovered that at high wind speeds, the sea surface c_d does not increase linearly. Rather, once a certain threshold is reached, it becomes suppressed or even reduced [28]. Laboratory findings have additionally verified the occurrence of this phenomenon [17]. Nonetheless, various studies showed variations in the c_d attenuation level at great wind speeds. A significant factor contributing to this variation is the lack of clarity in identifying the underlying mechanisms responsible for the observed attenuation. According to the research [29], the presence of waves reduces the ocean surface drag at great wind speeds. Actually, the surface of the ocean consists of not only ocean surface waves but in conjunction with spray droplets created by breaking waves, which float over the surface as the speed of the wind rises. During great wind speeds, spray droplets from the ocean are vital for interchange of momentum at the ocean surface thus, seeing them as a major factor in reducing the c_d [30,31]. Facts guiding the part of ocean spray droplets in decreasing sea surface drag at great wind speeds has been provided by experiments and observations [28].

As wind speed rises, waves in high-wind conditions break, producing a multitude of tiny spray droplets. These plentiful droplets, which linger in suspension above the surface of the sea, play a part in creating a notable momentum flux known as the sea spray flux. It was also emphasized [26] that the flux of ocean spray from ocean surface spray at great wind velocities significantly affects a total exchange of momentum in the interface between the sea and air. As previously explained, it is evident that droplets from ocean spray add to decrease in the ocean drag on the sea surface under great wind speed situations within the ocean-atmosphere boundary layer.

The research [32] put forth an explanation, proposing that the availability of the sea spray flux accounts for the decrease in the sea surface c_d at high wind speeds. When sea sprays get into the air, their immediate acceleration by ambient winds follows. This phenomenon pertains to air movement on a small scale within a particular region or localized area. As a result, the wind velocity diminishes because of the discharge of this power. When the droplets from the spray re-impact the surface of the sea, they send their momentum back to the water. This procedure helps to redistribute momentum in-between the air and ocean at the boundary between the atmosphere and ocean. At wind velocities exceeding 30-35 m/s close to sea surface, the flux of momentum from ocean spray gets comparable with overall momentum flux at the interface between the air and sea. The research [32] states that above wind speeds of 60 m/s, the flux of momentum from ocean spray fully accounts for the air momentum flux. The c_d of great wind velocities was earlier computed relative to the total momentum flux created by the wind. Standing scientific expressions are available for the c_d at great wind velocities that accounts for this attenuation scenario [32].The c_d at great wind speeds was obtained by considering the rectification effect of the flux of momentum from ocean spray on the overall momentum flux at the interface between the air and ocean, and by explicitly including the appearance of ocean spray flux in the drag relationship [32]. It was concluded that the c_d does not keep increasing with wind speed at great speeds; rather, it diminishes. Accordingly, there was suggestion to critically look into how ocean spray droplets influence the drag in conditions of great wind speeds.

It is generally a known fact that ocean spray droplets make the drag to attenuate at great wind velocities. Notwithstanding, the expression of the sea spray generation function (SSGF), that measures the rate of growth of spray droplets per unit area and time has been a

subject of ongoing debate [33]. Due to this ambiguity, it is so hard to ascertain the precise extent of ocean spray droplets' contribution to the c_d attenuation. As per the analysis of previously suggested SSGFs, the results from SSGF calculations should roughly demonstrate a fourth-power dependence on friction velocity [34]. They established the state of magnitude for different SSGFs and noted three possible functions [34] that align with the known properties of sea spray creation. Nevertheless, of great importance is to emphasize that these functions do not consider the effect of surface waves. At the ocean–atmosphere boundary, waves frequently arise and are essential for transferring energy in-between these environments. In the meantime, the formation of ocean spray droplets is impacted by both the wind and significantly by wave states [31,35]. When wind speeds are high enough, the power of breaking waves rises, and thereby leading to the creation of droplets of ocean spray. These droplets are powerfully thrown out from the wave tops, and the devastating waves create a spray when they hit the water underneath [36,37]. Therefore, SSGFs that do not consider wave effects are insufficient. The research [38] integrated wave information into the SSGF through a parameterization method, dividing it into a bi-components: the spray droplet creation rate based on wave situations and the spray magnitude spectrum. Nevertheless, of note is the formulation by the research [38] which applies to spray droplets confined to a specific radius limit. The research [26] reported a new SSGF that consists of the impact of wave states on spray flux, building upon this work. They underscored the importance of taking wave conditions into account when calculating momentum flux from sea spray, emphasizing that it must not be overlooked. To sum up, the combined effects of wind and waves during sea spray generation are not sufficiently considered by current SSGFs. These functions require refinement to cover a wider limit of spray droplet radii affected jointly by wind and waves.

The research [9,39] used large-frequency velocity measurements to assess perturbations and obtained new hydrodynamic data 40 m from an offshore wind farm monopile during a spring-neap cycle. They see a traditional depth-limited boundary layer outside the wake, where shear of tides at the seabed forces significant perturbation creation and dissipation. Throughout the entire water column, disorder creation, dissipation, and stress are elevated in the wake; however, these effects are especially evident in the upper half, where they match up to a considerable mean speed shortage. The outcome of their research indicate that the eddy viscosity increases by a factor of ten, which signifies enhanced mixing within the water column. Meanwhile, the seabed drags coefficient doubles from to, demonstrating increased mobility at the seabed. This research provides valuable insights as offshore wind farms utilize both bottom-fixed and floating structures to venture into deeper, seasonally stratified waters. In regions with low background mixing rates, the introduction of enhanced wake turbulence may lead to far-reaching consequences.

The research [40] showed that a systematic examination of five parameterizations for the wind stress uncovers irregularity in the effectiveness of momentum segmentation that is dependent on the scheme, particularly in typhoon situations. Their findings expressed the impact of wind stress c_d formulation on the feedback between the atmosphere and ocean, demonstrating that wave-state aware algorithms provide better surge forecast correctness than methods that rely heavily on wind speed. Specifically, the increase in both the atmospheric bottom and sea surface stress due to a higher wind stress c_d results to larger sea surface currents, storm surges and less powerful winds. Their results gave practical idea for promoting operational marine forecasting scheme, as well as guidelines regarding the sensitivity and performance of different air-sea coupled models.

The parameterization is particularly crucial over Aiyetoro, a riverine location in the Ilaje Local Government Area of Ondo State, Southwest Nigeria, because of the area's susceptibility to coastal erosion, flooding, and climate change effects. It is essential to comprehend how wind-wave interactions work and the pattern in which they change the ocean surface drag in order to devise efficient coastal protection measures and sustainable development strategies for this area. There have been few or no reports of work on the modeling

c_d in the study area. Nonetheless, it plays a crucial role in onshore organization and marine works. This study therefore intends to statistically evaluate the yearly, seasonal, and monthly performances of various parameterizations of [2-6] under low wind conditions in the study area, using variables such as the cd, u*, c_p, R_B, α, u_{10} , hs and lp.

Section 2 outlines the data source and parameterization methods employed in estimating the sea surface c_d for the research site. The aforementioned section gives a detailed description of data sources, such as the ERA5 reanalysis dataset, and the specific parameterization schemes used to compute the c_d. The results of the analysis are then discussed in section 3, which examines the temporal variability, trends, and seasonal patterns of the c_d. Also, the statistical comparison among the parameterization schemes are stated and explained. In all, section 4 briefs the key research results and conclusions drawn from the study.

Study Area

Aiyetoro with coordinates of latitude 6.1°N and longitude 4.8°E and which is based in Ilaje Local Government Area of Ondo State, Southwest Nigeria, is the research area. Ilaje Area is coastal environs that spans three thousand square kilometers and is located between 4.349948° and 5.149688° East of the Greenwich meridian and 5.842676° and 6.682662° North of the Equator (**Figure 1**). Aiyetoro is a low-lying region that ends at the Atlantic Ocean's shore and is made up of multiple Niger River tributaries. It is made up of around 2.0 km of shoreline, multiple rivers and estuaries, and a stagnant mangrove swamp. The topography of Aiyetoro region is lowered about the sea by land subsidence, which also causes a significant rise in relative sea level.

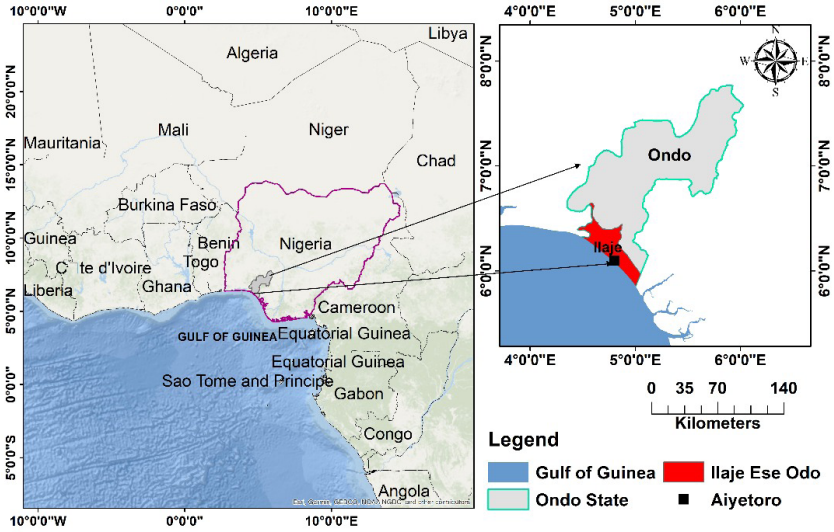

Figure 1. Study Map of Aiyetoro Community.

The tropical environment has two primary seasons: the rainy season, which lasts about seven months (from April to October), and the dry season, which lasts roughly four months (from November to March) [41]. The coastal regions of the area are typically characterized by rainforest type flora, with a profusion of trees and grasses along riverbanks. High-energy waves characterize the environment, leading to constant sea incursions into populated regions [42]. The study area's hydrological conditions are reliant on the Niger River, draining a considerable part of West Africa with water rich in sediment that flows into the Atlantic Ocean via 14 principal river outlets [43].

The region's predominantly flat and low-lying topography makes it especially susceptible to coastal erosion and flooding, particularly at high tide [44].

The coastal region of Ondo state, where the study site is located, is characterized by significant rainfall, which ranges from approximately 2,000 mm per year in the surroundings of Irele and Okitipupa to around 3,000 mm per year in the areas of Ilaje and Ese-Odo [45]. The Coastal Plain sands form the primary shallow hydro-geological units within this region. Typically, aquifers consist of continental sands, gravels, or marine sands. The

lateritic soil above the sands, together with the underlying non-permeable clay/shale from the Akinbo Formation, forms a protective arrangement for the aquifer units [46]. The surface geology of the study area consists of the Benin formation and recent alluvium. Due to the loose and heterogeneous characteristics of the Benin formation, the water table is found at a considerable depth that exceeds the reach of most typical hand-dug wells [47].

2. Data Source and Methodology

This study will utilize the ERA5 reanalysis data from the European Centre for Medium-Range Weather Forecasts (ECMWF) as its main data source. ERA5 provides one (1) hourly averaged estimates of several ocean-wave, atmospheric and land-surface quantities thus, providing a thorough overview of the Earth's climate and weather over several decades, with data dating back to 1940. ERA5 was chosen due to its demonstrated significance in African regions, as noted in earlier studies. The dataset is trustworthy and current, offering hourly, synoptic, daily, and monthly data segments for trend analysis as well as ocean weather monitoring and forecasting, especially in areas lacking sufficient data such as Africa [48].

The numerical model yields uninterrupted and dependable oceanic datasets across both space and time in open oceans. It is often employed to evaluate wind and wave climatology, as well as to conduct long-term analyses of the consequences of climate change on the wave climate [49]. The extensive historical data, along with its temporal coverage and spatial resolution, make it appropriate for examining the dynamics of ocean surface drag in the study location.

One hourly averaged values of parameters such as cd, u*, Tp, u10, hs, and lp were got from ERA5 Reanalysis for a period of 71 years (1950–2020) at https://cds.climate.copernicus.eu/user. The data were downloaded from a box ranging from 4.3° to 5.15° East of the Greenwich meridian and 5.8° to 6.7° North, with a spatial grid resolution of 0.5° × 0.5° and which contains nearshore and shore regions of the study location. The Linux operating system and MATLAB program were used to make a point extract of the aforementioned parameters for the study location.

2.1.Data Extraction

The Ondo state coastal region is located between latitudes 5.83°N to 6.3°N and longitudes 4.3°E to 5.08°E [50]. A program called RANDOM is written on MATLAB to random select many coordinate points within the study region. We selected 15 points:

Below is the program.

```
A = 4.3; B = 5.08;
Lon = A + (B – A)*rand(15,1);
A = 5.83; B = 6.3;
Lat = A + (B – A)*rand(15,1);
Lonlat = [lon,lat];
```

Data extraction script was written in accordance to the randomly selected points and was taken to Linux operating system for regional extraction for example, of the significant wave height (SWH) all through the study period. One hourly values of the SWH for normal years has 8760 data points, while for leap years has 8784 data points all through the study years.

```
use 1950.nc
list/file=station1.dat/clobber SWH[x-=4.94,y=5.89,l=1:8760]
list/file=station2.dat/clobber SWH[x-=5.00,y=6.02,l=1:8760]
list/file=station3.dat/clobber SWH[x-=4.4,y=6.26,l=1:8760]
list/file=station4.dat/clobber SWH[x-=5.01,y=6.2,l=1:8760]
list/file=station5.dat/clobber SWH[x-=4.79,y=6.28,l=1:8760]
list/file=station6.dat/clobber SWH[x-=4.38,y=6.14,l=1:8760]
list/file=station7.dat/clobber SWH[x-=4.52,y=5.85,l=1:8760]
list/file=station8.dat/clobber SWH[x-=4.73,y=6.23,l=1:8760]
list/file=station9.dat/clobber SWH[x-=5.05,y=6.27,l=1:8760]
list/file=station10.dat/clobber SWH[x-=5.05,y=6.15,l=1:8760]
list/file=station11.dat/clobber SWH[x-
```

=4.42,y=6.19,l=1:8760]

list/file=station12.dat/clobber SWH[x-=5.06,y=6.18,l=1:8760]

list/file=station13.dat/clobber SWH[x-=5.05,y=6.01,l=1:8760]

list/file=station14.dat/clobber SWH[x-=4.68,y=6.14,l=1:8760]

list/file=station15.dat/clobber SWH[x-=4.92,y=5.91,l=1:8760]

where x and y are respectively the longitudes and latitudes.

Out of the 15 randomly selected locations, the extraction tool extracted for a location (x = 4.79, y = 6.09, l = 1:8760) that is closest to Aiyetoro and was chosen for data analysis.The same extraction process was repeated for the rest parameters such as cd, u*, T_p, u_{10} and lp.

In Linux Environment (desktop):

*create a folder named data

*copy and paste (ERA 5 Reanalysis).nc files and extraction script into the folder

*open the data folder, right click and select open in terminal

*type conda activate FERRET

*type pyferret

*type use 1950.nc (for example)

*type sh d

*type go Extract.jnl

*data are now extracted based on the point coordinates in the script used.

*water points are the .dat files with data values in them.

*data in .dat format are now taken to MATLAB computational software and matlab script is written in line with the data from water points.

An example is attached below:

Filename = 'station1.dat';

Delimiterln = ':';

Headerlinesln = 7;

dat = importdata(filename,delimiterln,headerlinesln);

location1 = dat.data;

and so on to the 15th station.t1table(location1,location2,location3,location4,location5); etc and so on to location 15.

SWH 1950 = table2array(t1);

2.2.Statistical Tests of Performance

In accessing the predictive capabilities of the parameterizations, three statistical methods were employed. They are the root mean square error which is RMSE, mean bias error which is MBE and the correlation coefficient which is R. They are each defined in the research [51] as:

$$cc = \frac{\sum_{i-1}^{n}(a_i - \bar{a})(b_i - b)}{\sqrt{\sum_{i-1}^{n}(a_i - \bar{a})^2 \sum_{i-1}^{n}\left(b_i - \bar{b}\right)^2}} \quad (1)$$

$$Bias = b - \bar{a} \quad (2)$$

$$RMSE = \sqrt{\frac{1}{N}\sum_{i-1}^{n}(b_i - a_i)^2} \quad (3)$$

Note that a_i represents the ERA5 Reanalysis data for c_d, b_i represents the estimated data for c_d, a and b are the mean values of ERA5 data with the estimated data and the overall number of observations is denoted as N.

By enabling a detailed comparison of the actual discrepancies between parameterized values and those from the ERA5 Reanalysis, the root mean square error provides insights into the models' short-term effectiveness and performance. Because the RMSE cannot be negative, a value of zero indicates an ideal situation in which the parameterized values and the observed values are identical [52]. Considering that what constitutes an acceptable RMSE value is not definitive but depends on the particular context and the specific features of the datasets being analyzed. Conversely, the mean bias error test reveals the long-term performance of the models, showing whether values have been systematically overestimated or underestimated over a prolonged period.

An MBE value obtained by averaging the differences between parameterized and ERA5 Reanalysis values indicates whether there is a systematic overestimation or underestimation. The correlation coefficient (cc) evaluates how strong and in what direction the linear relationship is between the parameterized values and those from the ERA5 Reanalysis. A correlation coefficient closer to 1 indicates that the parameterization

more accurately reflects the variability in the c_d.

In general, a low MBE is desirable [53,54]. For better estimation, MBE and RMSE should be closer to zero, while r should be closer to unity [52].

For each of the five parameterizations, these error analyses were conducted in relation to the ERA5 Reanalysis and parameterized values of the c_d, on a yearly, seasonal, and monthly basis.

2.3.Linear Parameterization of c_d

A good number of models already exist for computing the ocean surface drag. Traditionally, the drag was thought to depend solely on wind speed, often represented by linear or quadratic relationships [14]. The sophistication of the interface between the air and sea, however, may require a more nuanced approach to accurately capture the variability and dependencies of this vital parameter. It is noteworthy that when more parameters are taken into account, wind speed continues to be the most influential factor by far. A method for linear parameterization consists of integrating wave-related parameters into the formulation of the c_d. Utilizing wave models to offer data on wave period, height and direction makes this achievable. Although linear parameterization provides a simplified method for representing the c_d, we recognize its limitations, as the relationships between the c_d and environmental parameters can be nonlinear, especially under extreme conditions. The quality and representativeness of the data utilized to derive the regression coefficients have a significant impact on the accuracy of the parameterization. Still, the linear parameterization serves as a useful means of enhancing estimates of air-sea momentum exchange, particularly in situations where computational resources are scarce or where a straightforward and efficient c_d representation is necessary.

Five parameterizations from existing models by some authors have been used to estimate c_d. These parameterizations are presented in **Table 1**.

Table 1. Parameterizations Used for this Study.

Equation	References	Parameterization
4	[2]	$c_d = 0.00078\left(\frac{c_p}{u_0}\right)^{-2/3}$
5	[3]	$c_d = \left(0.78 + 0.475\alpha^{1/2}u_{10}\right)*10^{-3}$
6	[4]	$c_d = 7.4*10^{-4}R_B^{\,0.08}$
7	[5]	$c_d = 2.5*10^{-3}\delta^{0.64}R_B^{\,1/6}$
8	[6]	$c_d = \left(0.75 + 0.07u_{10}\right)*10^{-3}$

where $c_p = {gT_p}/{2pi}$, $R_B = u*^2\,\omega pv$, $\omega p = 2pi/Tp$, v = 0.0000148, α = 0.0185 and $\delta = \frac{hs}{lp}$. *v signifies* the kinematic viscosity of air in m^2/s , the peak angular frequency is ωp in Hz, *the* acceleration due to gravity is g in m/s, c_p is the peak wave speed, R_B is the wind-sea Reynolds number, α is the Charnock coefficient, δ is the wave steepness, $u*$ is the wind friction velocity, T_p is the peak wave period, lp is the wave length, hs is the wave height and *pi* is 3.142. The above stated equations gave estimates for the years and for the wet season which runs from April to October and dry season, which spans from November through March.

3. Results

The monthly mean, range, and variability of cd and u10 over a seventy-one-year period are displayed in **Table 2**. November had the lowest monthly mean cd and u10, with values of 0.000825 and 3.38 m/s, respectively, and August had the highest values, with 0.001031 and 5.66 m/s, respectively. **Figure 2** explains the unimodal distribution between the 2 variables. Furthermore, the cd variability is lowest (63.24%) in November and highest (106.35%) in August. The variability for u10 is lowest in March (198.18%) and greatest in October (304.37%).

The annual, seasonal and monthly comparison between c_d from ERA5 and from authors are all displayed in **Figures 3–6**.

Table 2. Monthly Mean, Range and ariability of c_d and u_{10}.

	c_d			u_{10} (m/s)		
Month	**Mean**	**Range**	**Variability (%)**	**Mean**	**Range (m/s)**	**Variability (%)**
Jan	0.000884	0.00075	84.85	4.08	9.06	222.19
Feb	0.000927	0.00071	76.61	4.56	9.28	203.58
Mar	0.00094	0.000855	90.98	4.69	9.29	198.18
Apr	0.000911	0.000781	85.75	4.34	10.19	234.65
May	0.000858	0.00066	76.88	3.70	9.57	258.29
Jun	0.000884	0.000742	83.91	4.02	10.66	264.94
Jul	0.000993	0.000879	88.50	5.26	12.55	238.79
Aug	0.001031	0.001096	106.35	5.66	12.68	223.96
Sep	0.00094	0.000932	99.19	4.66	11.72	251.56
Oct	0.000846	0.000821	97.08	3.59	10.93	304.37
Nov	0.000825	0.000522	63.24	3.38	7.48	221.44
Dec	0.00085	0.000658	77.37	3.68	9.00	244.69

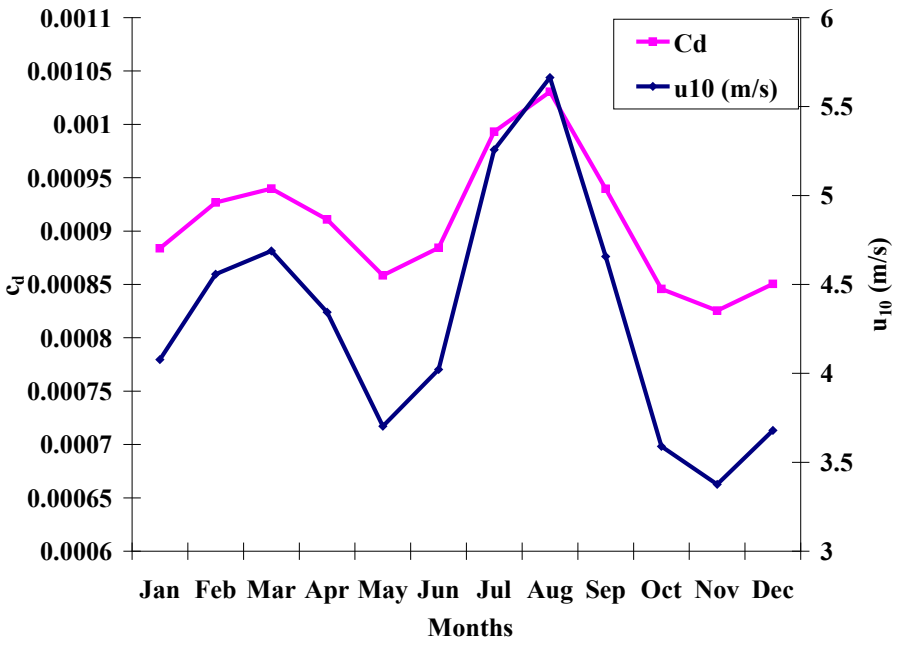

Figure 2. Monthly Pattern of c_d and $u_{10.}$

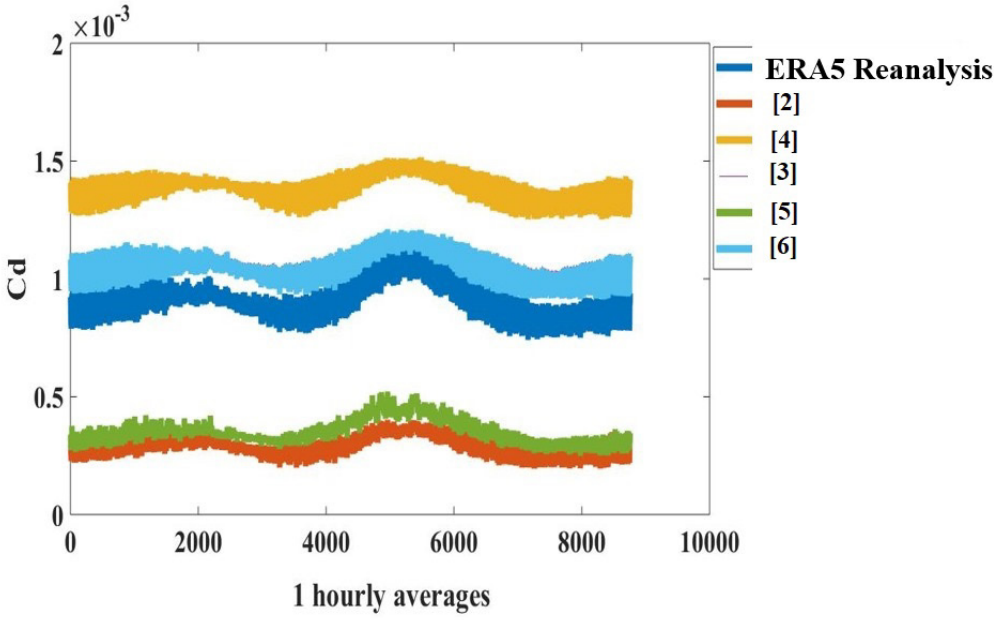

(**a**)

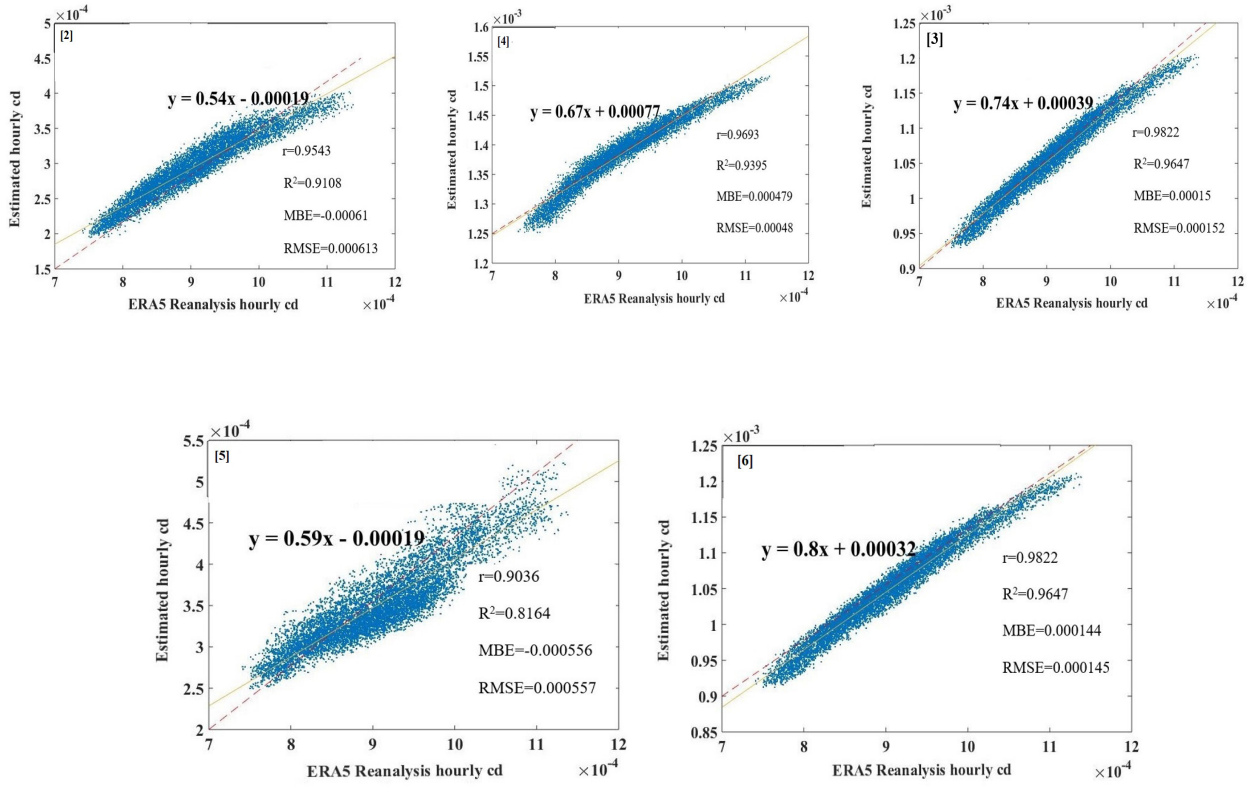

(**b**)

Figure 3. (**a**) Annual estimates of cd from the authors and (**b**) Corresponding XY scatter gram between ERA5 and estimated monthly mean hourly cd for the years.

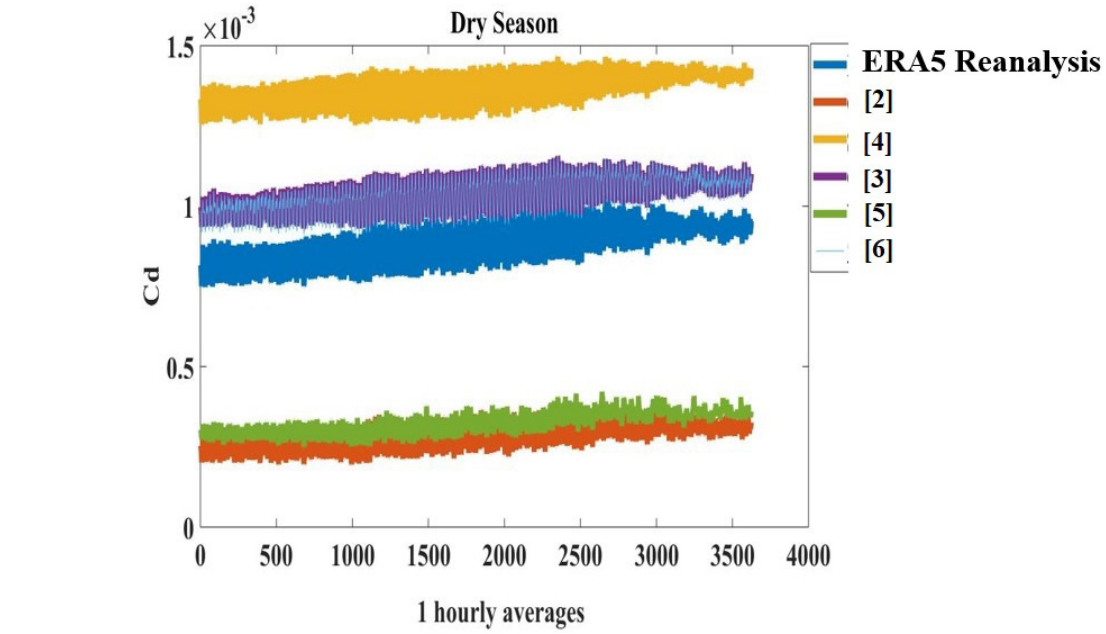

(**a**)

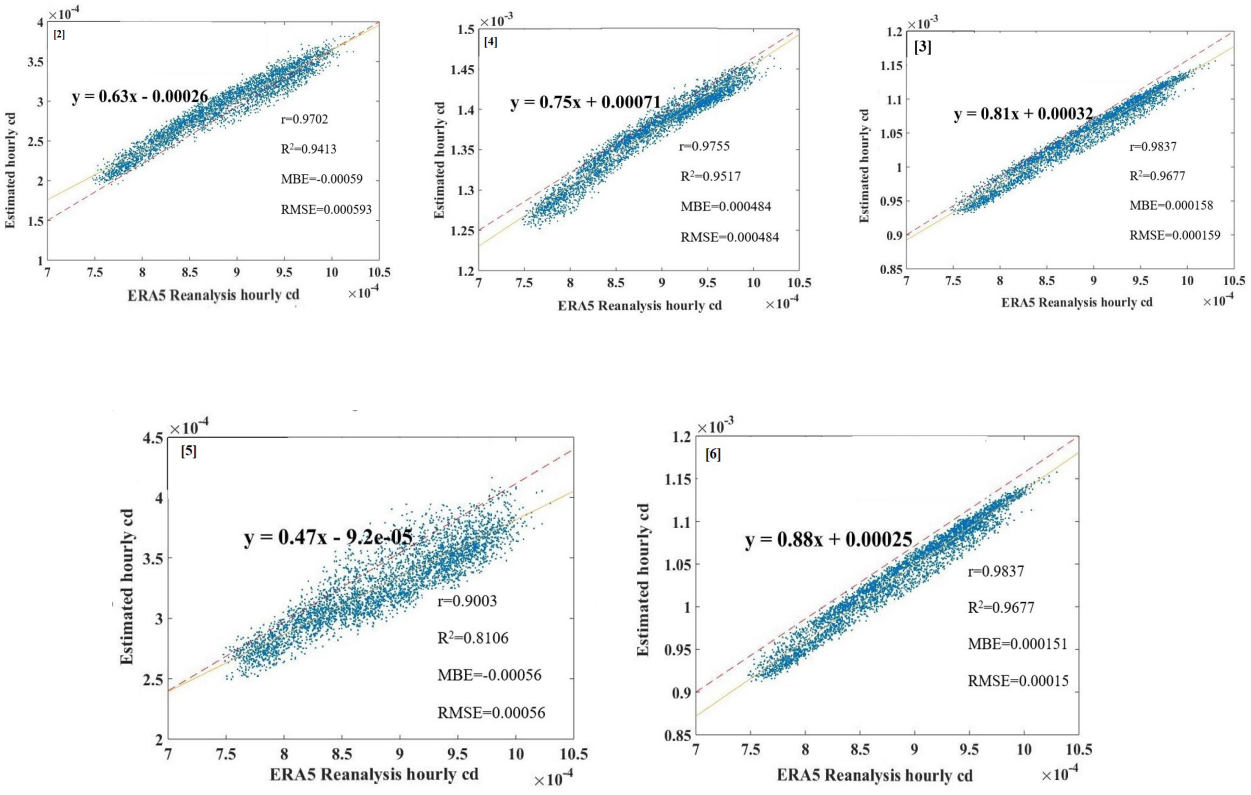

(**b**)

Figure 4. (**a**) Dry season estimates of cd from the authors and (**b**) Corresponding XY scattergram between ERA5 and estimated monthly mean hourly cd for the dry season.

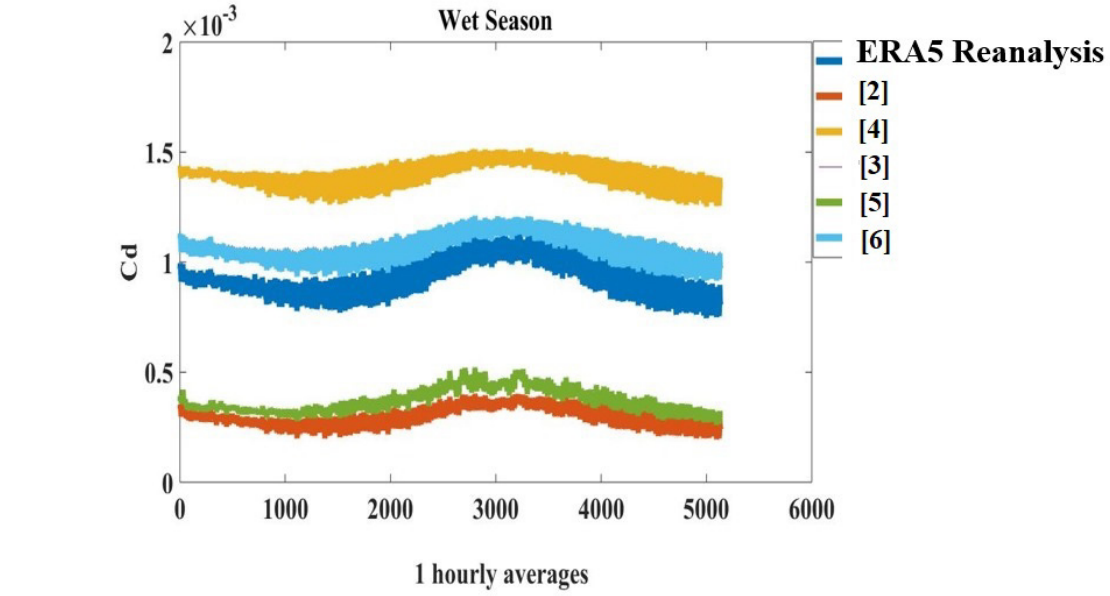

(**a**)

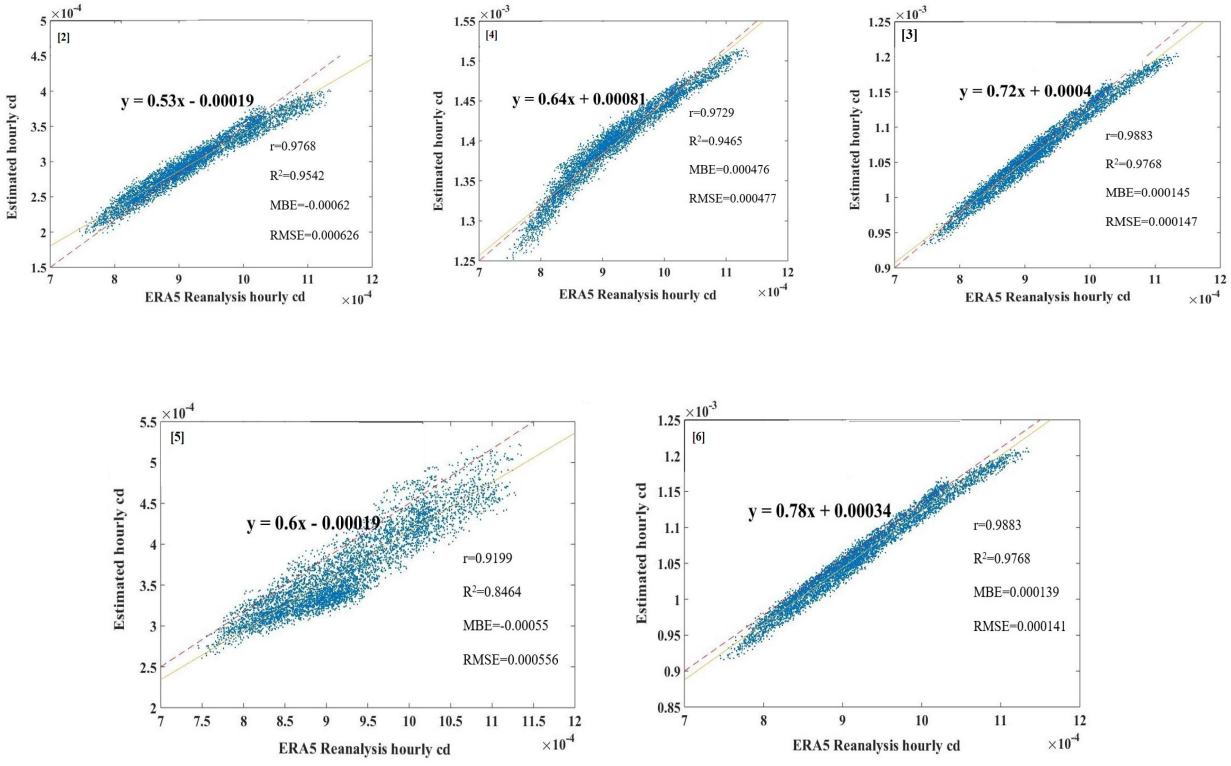

(**b**)

Figure 5. (**a**) Wet season estimates of cd from the authors and (**b**) Corresponding XY scatter gram between ERA5 and estimated monthly mean hourly cd for the wet season.

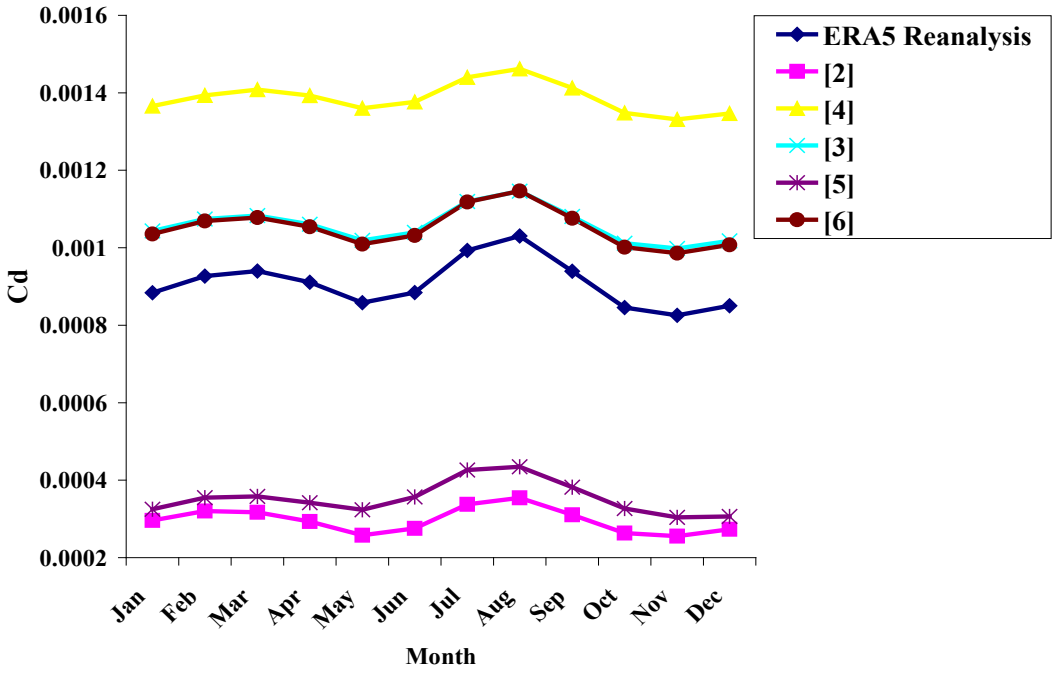

(**a**)

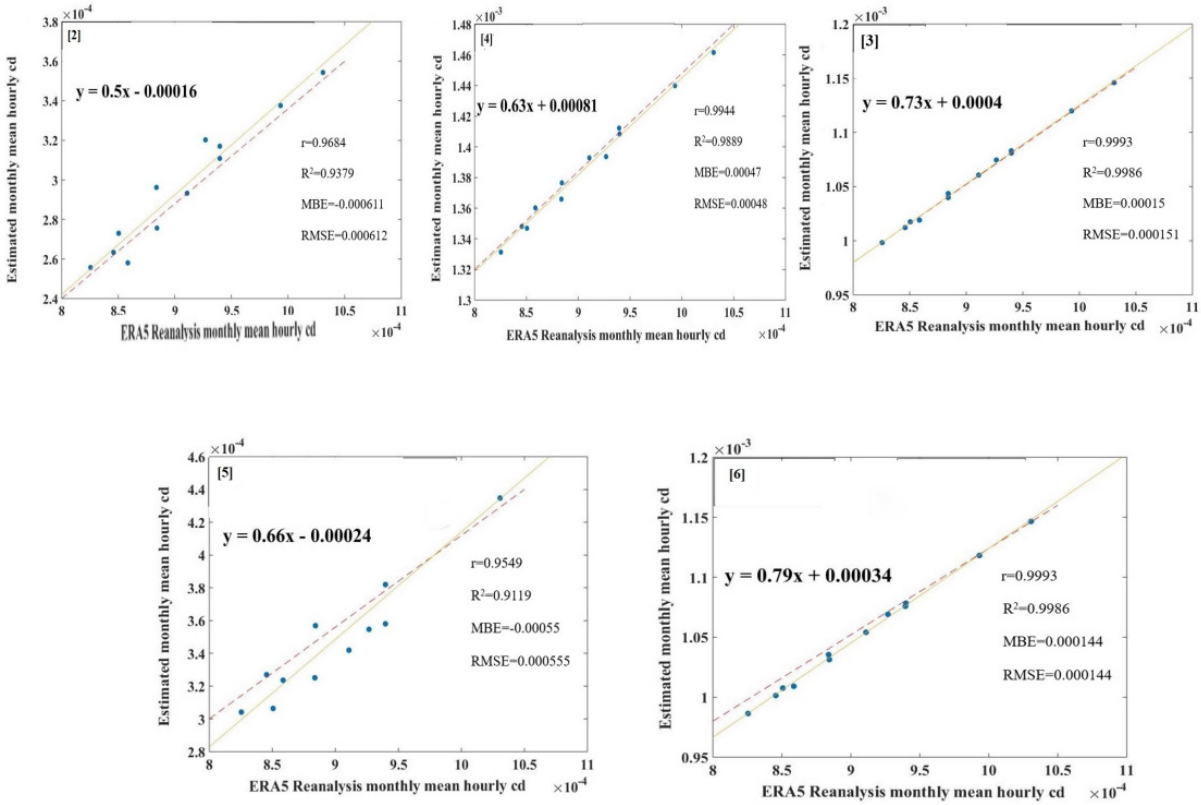

(**b**)

Figure 6. (**a**) Monthly estimates of cd from the authors and (**b**) Corresponding XY scatter gram between ERA5 and estimated monthly mean hourly cd.

Equations 4–8 have been used to estimate the cd. For the yearly and seasonal predictions of cd, one-hourly averaged values from ERA5 Reanalysis cd and from predictions were statistically evaluated for the RMSE, MBE, r, and R2. Also, the monthly predictions with the calculated RMSE, MBE, r, and R2 values are all presented in the scatter plots shown in **Figures 3b–Figure 6b**. The scatter plots showed that r differs amongst parameterizations, with greater values of r for [3 and 6] than the rest parameterizations.

Similarly, in an annual analysis as seen in **Figure 3b**, the parameterizations for [3 and 6] exhibit lower RMSE and MBE values than the other parameterizations. It follows that the parameterizations for the two authors performed better in predicting cd, and between these two, the parameterization for [6], with the lowest RMSE (0.000145) is the better choice for cd short-term performance in the study area. Nonetheless, for a long-term performance, the parameterization for [6], which has the least MBE of 0.000144 is to be preferred. The parameterizations of [2, 5] with respective MBE values of -0.00061 and -0.000556 underestimated cd, while those of [4, 3 and 6] with respective MBE values of 0.000479, 0.00015 and 0.000144 overestimated cd.

It is also obvious from the scatterplots of **Figure 3b** and **Figure 6b** that r is higher the time monthly estimates were used than when the actual annual one hourly data were used. Thus, cd showed superior performance with monthly values. The parameterizations for [3 and 6] had lower RMSE, MBE and higher r values in comparison with the rest parameterizations. The parameterization for [6], which had the lowest RMSE and MBE values of 0.000144 is to be chosen for both the short and long-term performances of cd at the study area. The cd is underestimated in the parameterizations of [2] (MBE = –0.000611) and [5] (MBE = –0.00055), while it is overestimated in the parameterizations of [6], (MBE = 0.000144), [3] (MBE = 0.00015) and [4] (MBE = 0.00047). The parameterization of [6] (r = 0.9986) and with the least RMSE and MBE values of 0.000144 best estimated cd. The scatterplots in **Figure 4b** and **5b** showed that r has a seasonal value with r being higher and MBE lower in the wet than the dry season, which implied that the equations generally performed better during the wet season. In this season, the parameterizations of [2 and 5] with respective MBE values of -0.00062 and -0.00055 underestimated cd, while the rest parameterizations overestimated cd. For the wet season, the parameterization by [6], which has the highest r value of 0.9883 and the lowest MBE and RMSE values of 0.000139 and 0.000141 respectively, is most effective for predicting cd in the study location.

4. Discussion

We conducted a statistical evaluation of the performance of some existing models for the cd over Aiyetoro in Ilaje Local Government Area, Ondo State, Southwestern Nigeria, by using one hourly data of some variables derived from ERA5 Reanalysis over a period of 1950–2020. The models are evaluated on a yearly, seasonal and monthly basis. Of all the tested models, the parameterization from [6], generally yielded better performance in estimating cd. The cd demonstrated superior performance with monthly values. For the seasonal prediction of cd, the equations performed better in the wet season.

5. Conclusion

In an attempt to quantify the exchange of momentum at Aiyetoro, Ilaje Local Government Area, Ondo State, Southwestern Nigeria, this work discussed the dependence of cd on the wave age, Charnock coefficient, wave steepness, wind-sea Reynolds number and 10m wind speed . The monthly average and variability of cd and u10 in the study location revealed that November had the least monthly average cd and u10, with values of 0.000825 and 3.38 m/s, respectively, and August had the highest values of 0.001031 and 5.66 m/s, respectively. Also, the cd variability is least (63.24%) during November and largest (106.35%) during August. The variability for u10 is least in March (198.18%) and largest in October (304.37%). Five models, were statistically tested for the predictive power of cd on an annual, seasonal and monthly basis over the study location.Of all the tested models, the parameterization from [6], generally yielded better performance in esti-

mating cd. Therefore, the cd given by [6] under low to moderate wind speeds is recommended for calculating air–sea momentum fluxes in the study location and its environs. Furthermore, the cd showed improved performance when using monthly values than when using annual and seasonal values. The equations yielded better performance in the wet season than in the dry season. Over the study area, the accuracy of sea surface stress calculations can be considerably enhanced in the future with the increase of observation data at low to moderate wind speeds. In addition, a new parameterization scheme that takes into account the impact of ocean current on the cd can enhance the theory of air-sea interaction and offer a precise air-sea momentum flux for modeling marine environments in ocean-atmosphere coupling models at low to moderate wind speeds.

Author Contributions

Conceptualization, A.A.O. and G.E.O.; methodology, A.A.O.; software, A.A.O..; validation, A.A.O., L.A.A. and P.C.; formal analysis, A.A.O.; investigation, G.E.O. and S.O.E.; resources, A.A.O..; data curation, S.O.E.; writing—A.A.O. and G.E.O.; writing—review and editing, A.A.O., G.E.O., S.O.E., L.A.A. and P.C.; visualization, A.A.O., L.A.A. and P.C.; project administration, S.O.E.; funding acquisition, L.A.A. and P.C. All authors have read and agreed to the published version of the manuscript.

Funding

This work was supported by Department of Engineering, University of Campania Luigi Vanvitelli, 81031 Aversa, Italy.

Institutional Review Board Statement

The study was conducted in accordance with the Declaration and approval by the Institutional Review Board of the Department of Engineering, University of Campania Luigi Vanvitelli, 81031 Aversa, Italy.

Informed Consent Statement

Informed consent was obtained from all subjects involved in the study.

Data Availability Statement

The data used for this research was sourced from the archive of https://cds.climate.copernicus.eu/user.

Acknowledgments

We authors deeply acknowledge the moral support of the Departments of Marine Science and Technology (MST) and Meteorology and Climate Science (MCS) for their encouragements towards the publication of this work. May the Departments continue to soar higher in all their endeavors.

Conflicts of Interest

The authors declare no conflict of interest. The funders had no role in the collection, analyses, or interpretation of data; in the writing of the manuscript; or in the decision to publish the results.

References

[1] Gao, Z., Wang, Q., Zhou, M., 2009. Wave-dependence of friction velocity, roughness length, and drag coefficient over coastal and open water surfaces by using three databases. Advances in Atmospheric Sciences. 26, 887–894. DOI: https://doi.org/10.1007/s00376-009-8130-7

[2] Shi, J., Zhong, Z., Li, R., et al., 2011. Dependence of sea surface drag coefficient on wind-wave parameters. Acta Oceanologica Sinica. 30(2), 14–24. DOI: https://doi.org/10.1007/s13131-011-0101-z

[3] Guan, C., Xie, L., 2004. On the linear parameterization of drag coefficient over sea surface. Journal of Physical Oceanography. 34, 2847–2851. DOI: https://doi.org/10.1175/JPO2664.1

[4] Wang, J., Song, J., Huang, Y., and Fan, C., 2013. On the parameterization of drag coefficient over sea surface. Acta Oceanol. Sin., 2013, Vol. 32, No. 5, P. 68-74 DOI: 10.1007/s13131-013-0315-3.

[5] Zhao, D., Li, M., 2018. Dependence of wind stress across an air–sea interface on wave states. Journal

of Oceanography. 75, 207–223. DOI: https://doi.org/10.1007/s10872-018-0494-9

[6] Charnock, H., 1955. Wind stress on a water surface. Quarterly Journal of theRoyal Meteorological Society. 81, 639–640. DOI: https://doi.org/10.1002/qj.49708135027

[7] Gao, Z., Zhou, S., Zhang, J., et al., 2021. Parameterization of Sea Surface Drag Coefficient for All Wind Regimes Using 11 Aircraft Eddy-Covariance Measurement Databases. Atmosphere. 12(11), 1485. DOI: https://doi.org/10.3390/atmos12111485

[8] Zhao, D., Li, M., 2024. Dependence of drag coefficient on the spectral width of ocean waves. Journal of Oceanography. 80, 129–143. DOI: https://doi.org/10.1007/s10872-023-00712-6

[9] Shi, J., Feng, Z., Sun, Y., et al., 2021. Relationship between Sea Surfacedrag coefficient and Wave State. Journal of Marine Science and Engineering. 9(11), 1248. DOI: https://doi.org/10.3390/jmse9111248

[10] Gao, Z., Peng, W., Gao, C.Y., et al., 2020. Parabolic dependence of the drag coefficient on wind speed from aircraft eddy-covariance measurements over the tropical Eastern Pacific. Scientific Reports. 10, 1805. DOI: https://doi.org/10.1038/s41598-020-58699-9

[11] Zhang, X., Bi, X., Gao, Z., et al., 2021. Parameterizations of drag coefficient and aerodynamic roughness length using the turbulence data collected during typhoons Hagupit and Chanthu. Journal of Tropical Oceanography. 40(2), 1–6.

[12] Zhou, X., Hara, T., Ginis, I., et al., 2022. Drag coefficient and its sea state dependence under tropical cyclones. Journal of Physical Oceanography. 52(7), 1447–1470. DOI: https://doi.org/10.1175/JPO-D-21-0246.1

[13] Hsu, J.Y., Lien, R.C., D'Asaro, E.A., et al., 2019. Scaling of drag coefficients under five tropical cyclones. Geophysical Research Letters. 46, 3349–3358. DOI: https://doi.org/10.1029/2018GL081574

[14] Shi, H., Li, Q., Wang, Z., et al., 2022. The Influence of Sea Sprays on Drag Coefficient at High Wind Speed. Journal of Ocean University of China. 22, 21–27. DOI: https://doi.org/10.1007/s11802-022-5050-y

[15] Kim, S-H., Kang, H-W., Moon, I-J., et al., 2022. Effects of the reduced air-sea drag coefficient in high winds on the rapid intensification of tropical cyclones and bimodality of the lifetime maximum intensity. Frontiers in Marine Science. 9, 1032888. DOI: https://doi.org/10.3389/fmars.2022.1032888

[16] Curcic, M., Haus, B.K., 2020. Revised Estimates of Ocean Surface Drag in Strong Winds. Geophysical Research Letters. 47(10), e2020GL087647. DOI: https://doi.org/10.1029/2020GL087647

[17] Takagaki, N., Komori, S., Suzuki, N., et al., 2012. Strong correlation between the drag coefficient and the shape of the wind sea spectrum over a broad range of wind speeds. Geophysical Research Letters. 39, L23604. DOI: https://doi.org/10.1029/2012GL053988

[18] Kuznetsova, A., Baydakov, G., Dosaev, A., et al., 2023. Drag coefficient Parameterization under Hurricane Wind Conditions. Water. 15(10), 1830. DOI: https://doi.org/10.3390/w15101830

[19] Hu, Y., Shao, W., Xu, Y., et al., 2024. Improvement of drag coefficient parameterization of WAVEWATCH-III using remotely sensed products during tropical cyclones. Ocean Dynamics. 74(10), 843–858. DOI: https://doi.org/10.1007/s10236-024-01638-3

[20] Feng, X., Sun, J., Yang, D., et al., 2021. Effect of drag coefficient Parameterizations on Air–Sea Coupled Simulations: A Case Study for Typhoons Haima and Nida in 2016. Journal of Atmospheric and Oceanic Technology. 38(5), 977–993. DOI: https://doi.org/10.1175/JTECH-D-20-0133.1

[21] Hwang, P.A., 2020. Impact on Sea-Surface Electromagnetic Scattering and Emission Modeling of Recent Progress on the Parameterization of Ocean Surface Roughness, Drag Coefficient, and Whitecap Coverage in High Wind Conditions. IEEE Journal of Selected Topics in Applied Earth Observations and Remote Sensing. 13, 1879–1887. DOI: https://doi.org/10.1109/JSTARS.2020.2977420

[22] Lin, S., Sheng, J., 2020. Revisiting dependences of the drag coefficient at the sea surface on wind speed and sea state. Continental Shelf Research. 207, 104188. DOI: https://doi.org/10.1016/j.csr.2020.104188

[23] Zhao, Z., Shi, J., Wang, H., et al., 2024. Parameterization scheme of the sea surface drag coefficient considering the influence of wave states and sea spray stress. Frontiers in Marine Science. 11, 1336709. DOI: https://doi.org/10.3389/fmars.2024.1336709

[24] Chen, S., Jiang, W.Z., Xue, Y., et al., 2024. A New Wave-State-Based Drag Coefficient Parameterization for Coastal Regions. Journal of Physical Oceanography. 54(3), 809–821. DOI:

https://doi.org/10.1175/JPO-D-23-0081.1

[25] Zhang, C., Chen, L., Brett, M.T., 2024. Adaptation of wind drag coefficient parameterization: Improvement of hydrodynamic modeling by a wave-dependent cd in large shallow lakes. Water Resources Research. 60, e2023WR035914. DOI: https://doi.org/10.1029/2023WR035914

[26] Shi, J., Zhao, D., Li, X., et al., 2009. New wave-dependent formulae for sea spray flux at air-sea interface. Journal of Hydrodynamics. 21, 573–581. DOI: https://doi.org/10.1016/S1001-6058(08)60186-9

[27]Rizza, U., Canepa, E., Ricchi, A., et al., 2018. Influence of wave state and sea spray on the roughness length: feedback on medicanes atmosphere. Atmosphere. 9(8), 301. DOI: https://doi.org/10.3390/atmos9080301

[28] Powell, M.D., Vickery, P.J., Reinhold, T.A., 2003. Reduced drag coefficient for high wind speeds in tropical cyclones. Nature. 422, 279–283. DOI: https://doi.org/10.1038/nature01481

[29] Moon, I.J., Ginis, I., Hara, T., et al., 2007. A physics-based parameterization of air–sea momentum flux at high wind speeds and its impact on hurricane intensity predictions. Monthly Weather Review. 135(8), 2869–2878. DOI: https://doi.org/10.1175/MWR3432.1

[30] Andreas, E.L., Emanuel, K.A., 2001. Effects of sea spray on tropical cyclone intensity. Journal of the Atmospheric Sciences. 58, 3741–3751. DOI: https://doi.org/10.1175/1520-0469(2001)058<3741: EOSSOT>2.0.CO;2

[31] Xu, X., Voermans, J.J., Ma, H., et al., 2021. A wind–wave-dependent sea spray volume flux model based on field experiments. Journal of Marine Science and Engineering. 9(11), 1168. DOI: https://doi.org/10.3390/jmse9111168

[32] Andreas, E.L., 2004. Spray stress revisited. Journal of Physical Oceanography. 34(6), 1429–1440. DOI: https://doi.org/10.1175/1520-0485(2004)034<1429: SSR>2.0.CO;2

[33] Lafon, C., Piazzola, J., Forget, P., et al., 2004. Analysis of the variations of the whitecap fraction as measured in a coastal zone. Boundary-Layer Meteorology. 111, 339–360. DOI: https://doi.org/10.1023/B:BOUN.0000016490.83880.63

[34] Andreas, E.L., Decosmo, J., 2002. The signature of sea spray in the hexos turbulent heat flux data. Boundary-Layer Meteorology. 103, 303–333. DOI: https://doi.org/10.1023/A:1014564513650

[35] Nilsson, E.D., Hultin, K.A.H., Mårtensson, E.M., et al., 2021. Baltic sea spray emissions: in situ eddy covariance fluxes vs. Simulated tank sea spray. Atmosphere. 12(2), 274. DOI: https://doi.org/10.3390/atmos12020274

[36] Lenain, L., Melville, W.K., 2017. Evidence of sea-state dependence of aerosol concentration in the marine atmospheric boundary layer. Journal of Physical Oceanography. 47(1), 69–84. DOI: https://doi.org/10.1175/JPO-D-16-0058.1

[37] Song, A., Li, J., Tsona, N., et al., 2023. Parameterizati ons for sea spray aerosol production flux. Applied Geochemistry. 157, 105776. DOI: https://doi.org/10.1016/j.apgeochem.2023.105776

[38] Zhao, D., Toba, Y., Sugioka, K., et al., 2006. New sea spray generation function for spume droplets. Journal of Geophysical Research Oceans. 111(C2), C02007. DOI: https://doi.org/10.1029/2005JC002960

[39] Austin, M.J., Unsworth, C.A., Van Landeghem, K.J.J., et al., 2025. Enhanced bed shear stress and mixing in the tidal wake of an offshore wind turbine monopile. Ocean Science. 21(1), 81–91. DOI: https://doi.org/10.5194/os-21-81-2025.

[40] Cai, L., Wang, B., Wang, W., et al., 2025. The Impact of Air–Sea Flux Parameterization Methods on Simulating Storm Surges and Ocean Surface Currents. Journal of Marine Science and Engineering. 13(3), 541. DOI: https://doi.org/10.3390/jmse13030541

[41] Ocean Energy Systems (OES), 2017. OES Annual Report 2017. Available from: https://www.ocean-energy-systems.org/publications/oes-annual-reports/document/oes-annual-report-2017/ (cited 13 December 2024).

[42] Soukissian, T., Karathanasi, F., Axaopoulos, P., 2017. Satellite-Based Offshore wind resource assessment in the mediterranean sea. IEEE Journal of Oceanic Engineering. 42(1), 73–86. DOI: https://doi.org/10.1109/JOE.2016.2565018

[43] Energiewende, A., Sandbag, 2018. The European Power Sector in 2017: State of Affairs and Review of Current Developments. Available online at: https://www.agora-energiewende.de/fileadmin/Projekte/2018/EU_Jahresrueckblick_2017/Agora_EU-report-2017_WEB.pdf (cited 16 January 2025).

[44] Onea, F., Ciortan, S., Rusu, E. 2017. Assessment of the potential for developing combined wind-wave projects in the European nearshore. Energy & Environment. 28(5–6), 580–597. DOI: https://doi.org/10.1177/0958305X17716947

[45] McMillan, D., Ault, G.W., 2010. Techno-economic comparison of operational aspects for direct drive and gearbox-driven wind turbines. IEEE Transactions on Energy Conversion. 25(1), 191–198. DOI: https://doi.org/10.1109/TEC.2009.2032596

[46] Liu, Y., Li, Y., He, F., et al., 2017. Comparison study of tidal stream and wave energy technology development between China and some Western Countries. Renewable and Sustainable Energy Reviews. 76, 701–716. DOI: https://doi.org/10.1016/j.rser.2017.03.049

[47] Fusco, F., Nolan, G., Ringwood, J.V., 2010. Variability reduction through optimal combination of wind/wave resources—an Irish case study. Energy. 35(1), 314–325. DOI: https://doi.org/10.1016/j.energy.2009.09.023

[48] Barbier, J., Guichard, F., Bouniol, D., et al., 2018. Detection of Intraseasonal Large-Scale Heat Waves: Characteristics and Historical Trends during the Sahelian Spring. Journal of Climate. 31(1), 61–80. DOI: https://doi.org/10.1175/JCLI-D-170244.1

[49] Bruno, M.F., Molfetta, M.G., Torato, V., et al., 2020. Performance Assessment of ERA5 Wave Data in a Swell Dominated Region. Journal of Marine Science and Engineering. 8(3), 214. DOI: https://doi.org/10.3390/jmse8030214

[50] Enikanselu, P.A., Balogun, A.A., Ewetumo, T., et al., 2025. Exploration of Wind-Wave Energy Potentials for Renewable Energy Development in Parts of Ondo Coastal and Offshore Locations, Southwestern Nigeria. Indian Journal of Energy and Energy Resources (IJEER). 4(2), 1–10. DOI: https://doi.org/10.54105/ijeer.B1039.04020225

[51] Wilks, D.S., 1995. Statistical Methods in the Atmospheric Sciences: An Introduction. Academic Press: San Diego, CA, USA. pp. 1–649.

[52] Osinowo, A.A., Okogbue, E.C., 2013. Estimating Global Solar Radiation from some Readily Measured Climatic Parameters over the Major Climatic Zones of Nigeria. Ife Research Publications in Geography. 12, 62–90.

[53] Iqbal, M., 1983. An introduction to solar radiation. Academic Press: New York, NY, USA. pp. 59–67.

[54] Halouani, N., Nguyem, C.T., Vo-Ngoc, D., 1993. Calculation of monthly average global solar radiation on horizontal surfaces using daily hours of bright sunshine. Solar energy. 50(3), 247–258. DOI: https://doi.org/10.1016/0038-092X(93)90018-J